An Investigation of Shear Instability in a Shallow Water

By Takehiko Satomura

Geophysical Institute, University of Tokyo, Tokyo
(Manuscript received 15 August 1980, in revised form 6 November 1980)

Abstract

The stability of parallel shear flows of a shallow fluid is investigated by linear analysis. Following Blumen (1970), a necessary condition for instability and the Howard semi-circle theorem are rederived for a shallow water, and energy equations are also derived. Then we examine the stability of two types of basic flows: plane Couette flow bounded in both sides (case I), and the same flow but unbounded in one side to connect with a rest fluid (case II).

By obtaining solutions expressed as power series, eigenvalues and eigenfunctions are determined to high accuracy. In the case I, it is shown that normal modes of gravity waves in a channel are modified by the basic shear flow to become unstable in some discrete ranges of the wavenumber, if Froude number, Fr, is greater than 2. In the case II, it is shown that two types of unstable waves are found for Fr>1: One is similar to the unstable waves in the case I but modified by the presence of the rest fluid. The wave is trapped near the boundary. The other is a wave destabilized by the shear too, but radiates its energy to the unbounded rest fluid. The unstable regions of the waves of this type are continuous in wave number space. The structure of all unstable waves found in this paper are similar to that of gravity waves.

It is shown that the unstable waves extract their energy not from the "ordinary" mean kinetic energy, but from an additional term of the mean kinetic energy arising from the correlation between perturbation zonal velocity and perturbation depth, and thus reduce the "depth-weighted" mean kinetic energy. Variation of the basic flow with time and some possibilities of redistribution of momentum by these unstable gravity waves are discussed.

Relation between our results and Blumen *et al.* (1975) is also commented.

1. Introduction

The purpose of this investigation is to examine the effect of horizontal divergence upon the stability of a parallel shear flow and to present a possible mechanism of excitation of gravity waves.

To investigate the effect of the divergence upon the barotropic instability, Lipps (1963) used a quasi-geostrophic flow with a jet ($U=\mathrm{sech}^2 y$) profile in a two-layered incompressible fluid. He obtained complex eigenvalues by analytical extension from an exact neutral solution, and found that both the β-effect and the divergence effect stabilize the flow. Philander (1976) studied a model similar to Lipps. His result was that both the β-effect and the divergence effect stabilize westerly jets, but both these effects destabilize easterly jets. Blumen (1970) discussed the stability of a compressible shear flow of a non-rotating fluid having a hyperbolic tangent profile, and also found reduction of growth rate by the divergence effect for Mach number $M \leq 1$. He also derived a necessary condition for instability: M (or Froude number $Fr) \geq 1$, or $U/U'' \leq 0$ in some region of fluid. The former condition relates with the effect of strong divergence and the latter condition relates with the existence of an inflection point (barotropic instability). Since he discussed only unstable waves for $M<1$, Blumen, Drazin and Billings (1975) extended the analysis to unstable waves for $M \geq 1$ in the same basic flow as Blumen (1970). An interesting finding of their work is that there exists another type of unstable waves which are thought to be acoustic waves generated in the shear zone and radiate outward. They called this type of unstable waves as second mode. Although they obtained such unstable waves for $M \geq 1$, and showed that they have non-

zero phase speed, they did not discuss the energetics or structure of the waves at all so that the nature of the waves remain unclear. Further, the coexistence of the inflection point instability makes the physical interpretation difficult. Whether the second unstable mode is linked with the point of inflection or not was not explored. One of the motivations of the present paper is to examine unstable travelling waves (gravity waves in a shallow water or acoustic waves in a compressible fluid) occuring in shear flow more comprehensively and to make their characteristics clear.

A number of studies on mechanisms of excitation of gravity waves by a horizontal shear, which is another motivation of this paper, were performed in context of the rain band formation in hurricanes. Among theoretical studies, Kurihara (1976) made a linear stability analysis using an approximation that both V (azimuthal velocity) and dV/dr of the basic state are constants. Although he found unstable out-going gravity waves, his model may be too much simplified to reach a definite conclusion of this instability problem. Willoughby (1977, 1978) treated a similar problem considering the variation of basic flow more strictly, and found that neutral forced waves grow spatially in outward propagation but their growth rates (spatial amplification rates) are not large enough to compensate geometrical spreading of cylindrical coordinates. Recently Broadbent and Moore (1979) studied the eigenvalue problem for a vortex in a homoentropic and compressible fluid for a wide range of M in the context of the noise generation from supersonic flows, and they found that acoustic waves which propagate to infinity are weakly unstable. Their model is similar to ours expect for the coordinates. But they did not discuss structure or energetics sufficiently.

These studies cited above suggest that horizontal shear flow may be unstable even if there is no inflection point, and that gravity waves may be excited. In connection with excitation of gravity waves, Blumen (1971) investigated the characteristics of disturbances in a two-dimensionally varying basic flow $U=(a+z)\tanh y$. He discussed unstable modes, but his discussion was confined to solutions which are valid only for $Fr\leq 1$. Thus, the unstable modes which he found are essentially barotropic instability.

It is rational to consider that unstable modes, related not with the point of inflection but with strong divergence, should be sought and their structures and energetics should be discussed in more detail. In this paper, two cases will be examined: case I is a Couette flow between two parallel walls, and case II is a Couette flow bounded only on one side and joined to a semi-infinite rest fluid. We consider only inviscid fluid. Froude number is greater than 1 for the both cases because these flows are stable for $Fr<1$ as shown in later section. Case I is treated for the purpose of finding a new unstable mode which has no relation with barotropic instability. In the non-divergence limit ($Fr\to 0$), Case (1960) showed that the perturbation equation for plane Couette flow has no normal modes (discrete-spectrum solutions) but only has continuous-spectrum solutions, which are "weak" solutions having a singularity at a critical point. He also showed that the basic flow is stable even if such a continuous solutions are used for expressing initial disturbances. Thus, if there exists an unstable discrete-spectrum solution in case I, it can not be connected with barotropic instability at all, but it should owe its existence to divergence (gravity wave). In fact, such unstable modes exist as will be shown in later section. On the other hand, case II is treated to examine radiative characteristics of the unstable gravity waves. We will find unstable out-going gravity waves and unstable trapped waves in the case II.

The present work has some interesting technicalities. Complex eigenvalues will be calculated down to ten decimal places by utilizing analytical solutions expressed by power series. The method used to obtain eigenvalues and eigenfunctions enables us to save computer resources and to evaluate them with any accuracy easily. The method is superior in that we never miss eigenvalues while we are free from the tedious work of omitting computational modes which are often mixed with the true eigenvalues if we use a finite difference method.

2. Basic equations

We shall consider the stability of a plane parallel flow, $U^*(y^*)$, of a shallow water where the basic flow U^* is in the x^* direction, and varies in the transverse direction, y^*. An infinitesimal disturbance having the velocity (u^*, v^*) in the (x^*, y^*) directions and a surface displacement h^* is superposed on this basic state.

It is convenient to non-dimensionalize the quantities by introducing a velocity scale U_0, and a length scale L, both of which are straightforwardly derived from the basic flow, and a

depth scale H which is the basic depth of the fluid. The dimensionless coordinates, time, velocity, and surface displacement are written as

$$(x, y)=(x^*, y^*)/L\,, \quad t=t^*U_0/L\,,$$
$$U=U^*/U_0\,, \quad (u, v)=(u^*, v^*)/U_0$$
$$h=h^*/H \tag{2.1}$$

The perturbation equations for disturbances in an inviscid shallow water (without Coriolis force) then become

$$\frac{\partial u}{\partial t}+U\frac{\partial u}{\partial x}+v\frac{dU}{dy}+\frac{1}{Fr^2}\frac{\partial h}{\partial x}=0\,, \tag{2.2}$$

$$\frac{\partial v}{\partial t}+U\frac{\partial v}{\partial x}+\frac{1}{Fr^2}\frac{\partial h}{\partial y}=0\,, \tag{2.3}$$

$$\frac{\partial h}{\partial t}+U\frac{\partial h}{\partial x}+\frac{\partial u}{\partial x}+\frac{\partial v}{\partial y}=0\,, \tag{2.4}$$

where $Fr=U_0/\sqrt{gH}$ is the Froude number, g is the gravity acceleration. Equations (2.2) and (2.3) are the momentum equations, and (2.4) is the mass conservation equation.

We assume a form

$$q=\hat{q}(y)\exp\{(ik(x-Ct)\}\,, \tag{2.5}$$

for each component q of the perturbation quantities, where k is a real wave number and $C=C_r+iC_i$ is the complex phase velocity. The complex eigenvalue C is determined under the condition that perturbation quantities satisfy the linear equations (2.2), (2.3) and (2.4) and appropriate boundary conditions.

Upon writing u, v, and h in the form as (2.5), we eliminate $\hat{u}$ and $\hat{v}$ to obtain a single equation for $\hat{h}$ as

$$(U-C)\hat{h}''-2U'\hat{h}'+k^2(U-C)\times\{Fr^2(U-C)^2-1\}\hat{h}=0 \tag{2.6}$$

where prime denotes differentiation with respect to y. Equation (2.6) becomes identical with (7) in Blumen (1970) for a perturbation in compressible fluid with shear when Fr is replaced by Mach number M as he pointed out.

The boundary condition at a rigid wall is written as

$$\hat{v}=\hat{h}'=0\,. \tag{2.7}$$

When the fluid is unbounded, we assume that U approaches a constant value outside the shear zone. Then from (2.6) we have the asymptotic form of a solution as

$$\hat{h}\sim\exp[\pm k\{1-Fr^2(U-C)^2\}^{1/2}y]$$
$$\text{as}\quad |y|\to\infty. \tag{2.8}$$

If a rest fluid extends in the outside the shear zone as in the case II, the solution of (2.6) in the region of the rest fluid is

$$\hat{h}=\exp[\pm k\{1-Fr^2C^2\}^{1/2}y]\,. \tag{2.8'}$$

We do not confine ourselves to 'subsonic' disturbances, that is, dimensional phase speed C_r^* can be greater than the velocity of the gravity waves $\sqrt{gH}$, so that $Fr^2C_r^2$ can be greater than 1. Thus, the radicant in the right-hand side of (2.8) or (2.8') can be either positive or negative, and accordingly, the solution is exponential or sinusoidal. We select a solution which decays away from the shear zone or a solution which expresses a wave radiating from the shear zone*. Such solution is appropriate to be used as a boundary condition for a solution in the shear zone.

3. Characteristics of the basic equation

Before obtaining solutions of (2.6) for specific flows, we shall discuss some properties of solutions of (2.6).

3.1 The Howard semi-circle theorem

Since (2.6) is the same form as (7) in Blumen (1970), the Howard semi-circle theorem (Howard, 1961) can hold, as Blumen (1970) has shown. Dividing (2.6) by $(U-C)^3$, multiplying by $\hat{h}^*$, the complex conjugate of $\hat{h}$, and then integrating, we have the following relation from the real part of the result,

$$0\geq\int_a^b\frac{U(U-U_{\max})}{|U-C|^4}dy=\int_a^b k^2Fr^2|\hat{h}|^2dy+\left\{\left(C_r-\frac{U_{\max}+U_{\min}}{2}\right)^2+C_i^2-\left(\frac{U_{\max}-U_{\min}}{2}\right)^2\right\}\int_a^b\frac{Qdy}{|U-C|^4}\,, \tag{3.1}$$

where boundaries are at $y=a$ and $y=b$; a and b may be infinite. $U_{\max}$ and $U_{\min}$ denote the maximum and minimum values of U, respectively, and

$$Q\equiv k^2|\hat{h}|^2+|\hat{h}'|^2\geq 0\,. \tag{3.2}$$

Since $k^2Fr^2|\hat{h}|^2\geq 0$, (3.1) implies

$$\left(C_r-\frac{U_{\max}+U_{\min}}{2}\right)^2+C_i^2\leq\left(\frac{U_{\max}-U_{\min}}{2}\right)^2. \tag{3.3}$$

This is the theorem stating that if there is a growing disturbance as eigensolution its eigenvalue C_r+iC_i should lie in a semi-circle on the complex plane, given by (3.3). This theorem is important not only from theoretical viewpoint

* In the case where C has an imaginary part, this latter condition becomes the same as the former one.

but in a practical procedure of searching for C in the complex plane. Thus we will use (3.3) to restrict the complex C plane in which we must search to find complex eigenvalues.

3.2 Necessary condition for instability

We derive a necessary condition for instability following Blumen (1970). The equation for the potential vorticity ω is derived from (2.2)~(2.4) as

$$\frac{\partial \omega}{\partial t}+U\frac{\partial \omega}{\partial x}=U''v \tag{3.4}$$

where

$$\omega\equiv\frac{\partial v}{\partial x}-\frac{\partial u}{\partial y}+U'h . \tag{3.5}$$

The perturbation energy equation is also obtained as

$$\frac{\partial}{\partial t}\iint\frac{1}{2}\left(u^2+v^2+\frac{h^2}{F_r^2}\right)dxdy =-\iint uvU'dxdy . \tag{3.6}$$

Now (3.4) is multiplied by $\omega U/U''$ and integrated over the whole domain to yield

$$\frac{\partial}{\partial t}\iint\frac{U}{U''}\frac{\omega^2}{2}dxdy=\iint\omega vUdxdy . \tag{3.7}$$

Upon rewriting ω on the right-hand side of (3.7) by using (3.5) we integrate by parts to obtain

$$\frac{\partial}{\partial t}\iint\left(\frac{U}{U''}\frac{\omega^2}{2}+Uhu\right)dxdy=\iint uvU'dxdy . \tag{3.8}$$

Addition of (3.6) and (3.8) gives

$$\frac{\partial}{\partial t}\iint\frac{1}{2}\left\{\frac{U}{U''}\omega^2+\frac{1}{F_r^2}(h+F_r^2Uu)^2+v^2 +(1-F_r^2U^2)u^2\right\}dxdy=0 . \tag{3.9}$$

This implies that the basic flow is stable if the following relations hold in the whole domain.

$$1-F_r^2U^2\geq 0 \quad\text{and}\quad \frac{U}{U''}\geq 0 . \tag{3.10}$$

In the dimensional form, (3.10) is

$$\sqrt{gH}\geq|U| \quad\text{and}\quad \frac{U}{U''}\geq 0 . \tag{3.10'}$$

Inequalities (3.10) or (3.10′) are the same as Blumen (1970)'s if Fr is replaced by M.

If we choose a coordinate system moving in the x-direction, the inequalities (3.10) and (3.10′) may change. But the physical properties must not change. From this consideration we see that a basic flow is stable if (3.10) or (3.10′) hold at least in one of the coordinate systems which are moving in the x-direction. Note that such a consideration leads to the stronger necessary condition for instability (Fjørtoft, 1950) concerning the barotropic instability.

3.3 Energetics

For discussing the energetics of the flow, dimensional form is convenient. The total velocity $(u^\dagger, v^\dagger)$ and the total depth $h^\dagger$ can be expanded in power series of a small parameter ε (to the second order) as

$$\begin{aligned} u^\dagger&=U+\varepsilon u+\varepsilon^2U^{(2)} ,\\ v^\dagger&=\varepsilon v+\varepsilon^2v^{(2)} ,\\ h^\dagger&=H+\varepsilon h+\varepsilon^2H^{(2)} , \end{aligned} \tag{3.11}$$

where all variables have dimensions and ε is a small parameter proportional to perturbation amplitude. U is the basic flow, H is the basic depth (constant), u, v, and h are the first order perturbations, and $U^{(2)}$, $V^{(2)}$, and $H^{(2)}$ express variations of the zonal mean quantities at the second order. So far as we are concerned with the energetics, we do not lose validity by considering only the zonal mean parts of the second order variables $U^{(2)}$, $V^{(2)}$, $H^{(2)}$.

'Local' kinetic energy, E_l, may be expanded as

$$\begin{aligned} E_l&=\frac{1}{2}(H+\varepsilon h+\varepsilon^2H^{(2)})\{(U+\varepsilon u+\varepsilon^2U^{(2)} +(\varepsilon v+\varepsilon^2V^{(2)})^2\}\\ &=\frac{1}{2}HU^2+\frac{\varepsilon}{2}(2HUu+hU^2)+\frac{\varepsilon^2}{2}\{2HUU^{(2)} +H^{(2)}U^2+2huU+H(u^2+v^2)\}+O(\varepsilon^3) . \end{aligned}$$

By taking the zonal mean of the above expression, we have

$$\begin{aligned} E&=\frac{1}{2}HU^2+\frac{\varepsilon^2}{2}\{2HUU^{(2)}+H^{(2)}U^2 +2\overline{hu}U+H(\overline{u^2}+\overline{v^2})\}\\ &=\frac{1}{2}HU^2+\varepsilon^2\left\{E_s+\left(E_p-\frac{g}{2}\overline{h^2}\right)\right\} , \end{aligned} \tag{3.12}$$

where a bar denotes averaging in the x-direction, and

$$E_s=\frac{1}{2}H^{(2)}U^2+HUU^{(2)}+\overline{hu}U , \tag{3.13a}$$

$$E_p=\frac{1}{2}H(\overline{u^2}+\overline{v^2})+\frac{g}{2}\overline{h^2} . \tag{3.13b}$$

The first term of the right-hand side of (3.12) is the basic kinetic energy, and E_p is the total energy of the perturbation per unit area. As

shown soon later, E_s is the kinetic energy of depth weighted zonal mean flow contained in a column with unit area. We are interested in the energy conversion between E_s and E_p, or, in a special case, among the terms in the right-hand side or (3.13a).

Now, the first-order perturbation equations are

$$\frac{\partial u}{\partial t}+U\frac{\partial u}{\partial x}+v\frac{dU}{dy}+g\frac{\partial h}{\partial x}=0\,, \tag{3.14}$$

$$\frac{\partial v}{\partial t}+U\frac{\partial v}{\partial x}+g\frac{\partial h}{\partial y}=0\,, \tag{3.15}$$

$$\frac{\partial h}{\partial t}+U\frac{\partial h}{\partial x}+H\left(\frac{\partial u}{\partial x}+\frac{\partial v}{\partial y}\right)=0\,, \tag{3.16}$$

and the second-order equations are

$$\frac{\partial U^{(2)}}{\partial t}+\overline{u\frac{\partial u}{\partial x}}+\overline{v\frac{\partial u}{\partial y}}+V^{(2)}\frac{dU}{dy}=0\,, \tag{3.17}$$

$$\frac{\partial V^{(2)}}{\partial t}+\overline{u\frac{\partial v}{\partial x}}+\overline{v\frac{\partial v}{\partial y}}+g\frac{\partial H^{(2)}}{\partial y}=0\,, \tag{3.18}$$

$$\frac{\partial H^{(2)}}{\partial t}+\overline{\frac{\partial hu}{\partial x}}+\overline{\frac{\partial hv}{\partial y}}+H\frac{\partial V^{(2)}}{\partial y}=0\,. \tag{3.19}$$

Multiplying (3.14), (3.15) and (3.16) by Hu, Hv and gHh respectively, adding the results, and integrating over the whole domain, we obtain

$$\frac{\partial}{\partial t}\int E_P dy=-\int H\overline{uv}\frac{dU}{dy}dy\,, \tag{3.20}$$

The right-hand side of (3.20) expresses the rate of energy conversion by the Reynolds stress. Multiplying (3.14), (3.16), (3.17), and (3.19) by Uh, Uu, HU, and $U^2/2$, respectively, integrating over the whole domain, and adding the results, we obtain

$$\frac{\partial}{\partial t}\int E_s dy=\int H\overline{uv}\frac{dU}{dy}\,dy\,. \tag{3.21}$$

The right-hand side of (3.21) expresses the rate of energy conversion by the Reynolds stress, and it is the quantity that causes change of the perturbation energy as seen in (3.20). Thus, the identification of E_s as the (weighted) zonal mean kinetic energy is appropriate.

Since, as shown in following sections, the last term in the right-hand side of (3.13a), huU, plays an important role, we divide E_s into two parts:

$$E_S=E_B+E_{BP}\,, \tag{3.22}$$

where $E_B=H^{(2)}U^2/2+HUU^{(2)}$ expresses the zonal mean kinetic energy arising from the second order zonal mean quantities, and $E_{BP}=\overline{hu}U$ is interpreted as additional part of the zonal mean kinetic energy due to the perturbation surface displacement. Then, equation (3.21) is divided as follows:

$$\frac{\partial}{\partial t}\int E_B dy=\int\left(HU\overline{u\frac{\partial v}{\partial y}}+\overline{hv}U\frac{dU}{dy}\right)dy+\int H\overline{uv}\frac{dU}{dy}\,dy\,, \tag{3.23a}$$

$$\frac{\partial}{\partial t}\int E_{BP}dy=-\int\left(HU\overline{u\frac{\partial v}{\partial y}}+\overline{hv}U\frac{dU}{dy}\right)dy\,. \tag{3.23b}$$

The first and the second integrals in the right-hand side of (3.23a) express the rate of the energy conversions to E_{BP} and E_P, respectively.

It is worth noting that, even if 'ordinary' zonal mean kinetic energy E_B does not change, perturbation energy can grow at the expense of the additional energy term E_{BP}, which may become negative. In fact, the linear shear flow, that we consider in detail in the next section, falls in this interesting case.

3.4 *Characteristics of solutions near the singular point*

Equation (2.6) has a singular point at $y=y_c$ where $U(y_c)=C$. To examine the characteristics of a solution near the singular point, $\hat{h}$ and U are expanded as follows

$$\hat{h}=z^\lambda\sum_{n=0}^{\infty}a_n z^n\,, \tag{3.24}$$

and

$$U=\sum_{n=0}^{\infty}\frac{z^n}{n!}U_c^{(n)} \tag{3.25}$$

where $z=y-y_c$, λ is the index which should be determined later and $U_c^{(n)}$ is the n-th order derivative of $U(y)$ at $y=y_c$. After substitution of (3.24) and (3.25) into (2.6), and rearrangement, we obtain the following equations for a's by using the fact that coefficient of each power of z should be zero;

$$U_c^{(1)}\lambda(\lambda-3)a_0=0\,, \tag{3.26a}$$

$$U_c^{(1)}(\lambda+1)(\lambda-2)a_1=-\frac{U_c^{(2)}}{2}\lambda(\lambda-5)a_0\,, \tag{3.26b}$$

$$U_c^{(1)}(\lambda+2)(\lambda-1)a_2=-\left\{\frac{U_c^{(3)}}{3!}\lambda(\lambda-7)-k^2U_c^{(1)}\right\}a_0-\frac{U_c^{(2)}}{2}(\lambda+1)(\lambda-4)a_1\,, \tag{3.26c}$$

$$U_c^{(1)}(\lambda+3)\lambda a_3=-\left[\frac{U_c^{(4)}}{4!}\lambda(\lambda-9)-k^2\frac{U_c^{(2)}}{2}\right]a_0$$

$$-\left[\frac{U_c^{(3)}}{3!}(\lambda+1)(\lambda-6)-k^2U_c^{(1)}\right]a_1$$
$$-\frac{U_c^{(1)}}{2}(\lambda+2)(\lambda-3)a_2\,, \qquad (3.26d)$$
.....

From (3.26a), we determine values of the indices as $\lambda=3$ and $\lambda=0$. The former gives a regular solution while adopting the latter we fail to determine a_3 as seen from (3.26d) and we have to seek for another independent solution by the method of Frobenius. Thus we have general solution as,

$$\hat{h}=Ah_{1(z)}+Bh_{2(z)}\,, \qquad (3.27)$$

where A and B are constants, and h_1 and h_2 are two independent solutions given as

$$h_1(z)=z^3\sum_{n=0}^{\infty}a_nz^n\,, \qquad (3.28)$$

$$h_2(z)=\alpha h_1(z)\log z+\sum_{n=0}^{\infty}b_nz^n\,, \qquad (3.29)$$

$$\alpha=-\frac{k^2U_c^{(2)}}{2U_c^{(1)}}\,. \qquad (3.30)$$

b_n are coefficients determined from the requirements that (3.29) satisfies (2.6); but their explicit forms may not necessarily be written here for the reason as explained soon later.

Although, in general, $\hat{h}$ has a logarithmic singularity at $y=y_c$ as (3.29) shows, $\hat{h}$ becomes regular in the whole domain if $U_c^{(2)}=0$, as seen from (3.30). This occurs either in the case where the shear is linear or in the case where we happen to have $U_c^{(2)}=0$ for non-linear shear. Most of the studies so far made deal with the latter case, because they consider only the so-called inflection-point instability. In this paper, however, we confine ourselves to the linear shear flow, because we are interested in destabilization of gravity waves and therefore it is desirable to avoid the occurrence of an inflection-point instability. In this case, $\hat{h}$ becomes a regular function.

4. Stability of linear shear flows

4.1 Notes for the necessary condition of a linear shear flow

When $U''=0$, the derivation of the condition (3.10) or (3.10′) is incorrect. But, as we will show subsequently, a similar condition can be obtained. The equation for the potential vorticity ω in the linear shear case is written formally as

$$\frac{\partial\omega}{\partial t}+U\frac{\partial\omega}{\partial x}=\gamma v\delta(y-y_d)\,, \qquad (4.1)$$

where γ is a constant and $\delta(y)$ is the delta function. This delta function is caused by a discontinuous change of $U'(y)$ at $y=y_d$ (for example, $y=0$ in the case II).

Since u, v, and h are assumed to have the form as (2.5), equation (4.1) is rewritten

$$ik(U-C)\omega=\gamma v\delta(y-y_d)\,. \qquad (4.2)$$

When U is a linear function of y, (4.2) means

$$\omega=0\,, \qquad (4.3)$$

except for $y=y_d$.*

Deviding (4.2) by $ik(U-C)$, multiplying by vU, and integrating over the whole domain, we obtain

$$\iint\omega vUdxdy=\gamma'U_dv_d^2 \qquad (4.4)$$

where $v_d=v(y_d)$ and $\gamma'=\gamma/ik(U_d-C)$.

Equation (4.4) is the same as (3.7) except for the left-hand side. Thus, similar calculation as before gives

$$\frac{\partial}{\partial t}\iint Uhudxdy=\iint uvU'dxdy$$
$$-\gamma'v_d^2U_d-[\overline{uv}]_{y_d}U_d\,, \qquad (4.5)$$

where $[\overline{uv}]_{yd}$ is a jump of the Reynolds stress, $\overline{uv}$, at $y=y_d$.

Adding (3.6) and (4.5), we have

$$\frac{\partial}{\partial t}\iint\frac{1}{2}\left[\frac{1}{F_r^2}(h+F_r^2Uu)^2+v^2\right.$$
$$\left.+(1-F_r^2U^2)u^2\right]dxdy$$
$$=-(\gamma'v_d^2+[\overline{uv}]_{y_d})U_d\,. \qquad (4.6)$$

When there is no discontinuity of U' as in the case I or $U_d=0$ as in the case II, the right-hand side of (4.6) is zero. In these cases, the above equation implies that the basic flow is stable if an inequality

$$1-F_r^2U^2\geq0\,, \qquad (4.7)$$

holds in the whole domain. In the dimensional form, (4.7) is written as

$$\sqrt{gH}\geq U\,. \qquad (4.7')$$

In the subsequent part of the present paper we treat stability of flows of two different profiles. Adopting the consideration in the last part of subsection 3.2 to (4.7) we obtain a necessary condition of instability as

$$F_r\geq2 \quad \text{for the case I.}$$

But, in the case II, that consideration cannot be

* Thus we excluded singular normal modes, $\omega=\delta(U-C)$, associated with continuous eigenvalues as obtained by Case (1960).

adopted, because (4.7) or (4.7′) is derived only for a coordinate system which gives $U_d=0$. Thus (4.7) is written as

$F_r \geq 1$ for the case II.

4.2 Case I: Plane Couette flow bounded in both sides

First we consider a plane Couette flow, *i.e.*, the fluid is bounded by rigid walls at $y=0$ and $y=1$, and the basic flow is a linear function of y:

$$U(y)=y\,. \tag{4.8a}$$

Then boundary conditions are

$$v=h'=0 \quad \text{at } y=0 \text{ and } y=1\,. \tag{4.8b}$$

This situation is schematically shown in Fig. 1*.

It is convenient to transform independent variable y into $z=U-C=y-C$. Then (2.6) becomes

$$z\frac{d^2\hat{h}}{dz^2}-2\frac{d\hat{h}}{dz}+k^2z(F_r{}^2z^2-1)\hat{h}=0\,, \tag{4.9}$$

and boundary condition (4.8b) is

$$v=\frac{d\hat{h}}{dz}=0 \text{ at } z=-C \text{ and } z=1-C. \tag{4.10}$$

To find solution of (4.9), $\hat{h}$ is expanded into power series of z as

$$\hat{h}=z^{\lambda}\sum_{n=0}^{\infty}a_nz^n\,. \tag{4.11}$$

Then from the preceding discussion (subsection 3.4) we see that both of the two roots of the indicial equation, $\lambda=0$ and $\lambda=3$, are valid and the general solution of (4.9) can be written as

$$\hat{h}=A\sum_{n=3(\text{odd})}^{\infty}a_nz^n+B\sum_{n=0(\text{even})}^{\infty}a_nz^n\,, \tag{4.12}$$

where A and B are constants, and (odd) or (even) means that the respective summation is carried out only for odd or even n's. The coefficients a's are determined as

$$a_0=1,\quad a_1=0,\quad a_2=-k^2/2,\quad a_3=1,$$
$$a_n=\frac{k^2(a_{n-2}+F_r{}^2a_{n-4})}{n(n-3)} \quad \text{for } n\geq 4\,. \tag{4.13}$$

The radius of convergence, ρ, of the power series is examined by use of the relation,

$$\rho=\lim_{n\to\infty}\frac{a_{n-2}}{a_n}\,, \tag{4.14}$$

and turns out to be infinity, so that (4.12) can be applied everywhere in the domain.

Now, an eigenvalue problem is formulated as follows: The boundary condition is (4.10). Then, substituting (4.12) into (4.10), we obtain,

$$A\sum_{n=3(\text{odd})}^{\infty}na_n(-C)^{n-1}+B\sum_{n=2(\text{evn})}^{\infty}na_n(-C)^{n-1}=0 \tag{4.15}$$

$$A\sum_{n=3(\text{odd})}^{\infty}na_n(1-C)^{n-1}+B\sum_{n=2(\text{even})}^{\infty}na_n(1-C)^{n-1}=0\,. \tag{4.16}$$

Requiring that A and B do not vanish, we have a characteristic equation for C as,

$$f(k,F_r\,;\,C)=\begin{vmatrix} f_1(-C) & f_2(-C) \\ f_1(1-C) & f_2(1-C)\end{vmatrix}=0, \tag{4.17}$$

where

$$f_1(z)=\sum_{n=3(\text{odd})}^{\infty}na_nz^{n-1}\,, \tag{4.18}$$

$$f_2(z)=\sum_{n=2(\text{even})}^{\infty}na_nz^{n-1}\,, \tag{4.19}$$

When k and Fr are given, (4.17) determines the eigenvalue C. Thus, to obtain an eigenvalue is equivalent to finding a zero point of the complex function $f(C)$. We seek eigenvalues by successive approximation as described below.

The basic idea of search is to use a theorem in complex function theory

$$N-P=\frac{1}{2\pi i}\oint_L\frac{df/dC}{f(C)}\,dC\,, \tag{4.20}$$

where $\oint_L dC$ means an integral along a closed contour L on the complex plane, and N and P are numbers of zero points and poles of the complex function $f(C)$ located in the domain enclosed by L, respectively. In the present case the two independent solutions of (4.9) are regular everywhere, so that their first derivatives f_1 and f_2 are regular and hence $P=0$. Equation (4.20) is transformed into a more convenient form

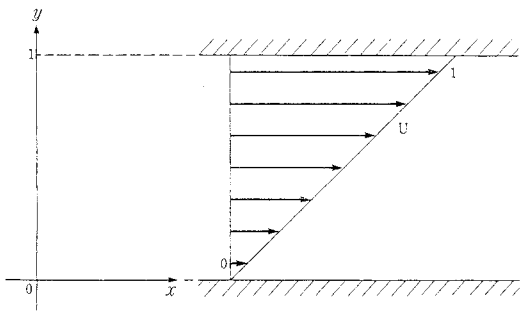

Fig. 1 The model of the case I. Non-dimensional width is 1 and non-dimensional basic flow varies from 0 to 1.

* All figures in this paper are drawn in the non-dimensional variables and amplitudes of perturbation variables are normalized by the maximum amplitude of h for each parameter.

$$N=\frac{1}{2\pi i}\oint_L d\log f=\frac{1}{2\pi i}[\arg(f_a)-\arg(f_b)]\,, \tag{4.20'}$$

where $Arg(f)$ is the argument of the function f, and f_a and f_b are the values of f at the fixed point on L after and before the line integration, respectively.

We search for the eigenvalues as follows:

(a) The parameters k and Fr are specified.

(b) f_a and f_b are evaluated numerically at a point on a rectangular contour L which includes the Howard semi-circle.

(c) If $N=0$, then another set of parameter values are given. But if $N=0$ we divide the rectangle into small sub-domains and f_a and f_b are re-evaluated at a point on the contour encircling every sub-domain. If we find N sub-domains which have a zero point, we repeat the procedure dividing the domain into smaller sub-domains until the domain in which C exists is so small that the iteration as described in (d) converges easily (see Fig. 2(a)).

(d) Divide the small sub-domain into M rectangles, each of which has the same area, and evaluate the left-hand side of (4.17), f, using the value of C's at each corner of the rectangles, c_1 to C_9 (see Fig. 2(b)). Then around the corner which gave the smallest absolute value of f, say C_9, make new M rectangles, each of which is $1/M$ of the rectangles of the first iteration, and re-evaluate f at new nine corners C_9–C_{17}. We repeat the procedure dividing the rectangle into M smaller rectangles and evaluating f using the values of C's at corners until the smallest absolute value of f is smaller than a specified value, say 10^{-10}. The approximate eigenvalue C is what makes $|f(C)|$ the smallest value.

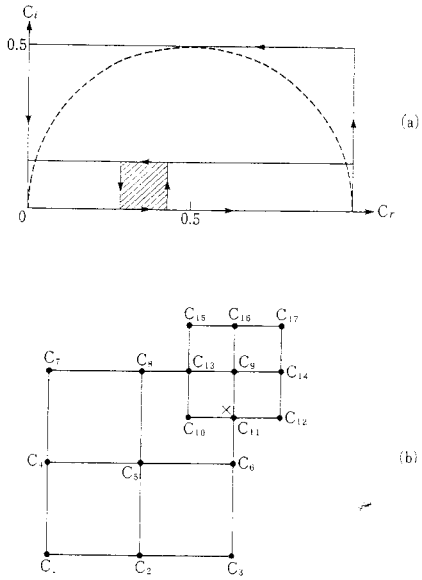

Fig. 2 Searching procedure for eigenvalues. (a) Dividing procedure. Line integral is evaluated along rectangles in the directions of arrows and shaded rectangular includes a zero point. (b) Iteration procedure for $M=2$. At first f's are evaluated at nine points C_1–C_9, then re-evaluated at nine points C_9–C_{17}. True eigenvalue locates at the point which is indicated by a cross, X.

Using a quadruple precision program, we obtain eigenvalues to more than ten places of decimals for all sets of parameter values. In order to get the above mentioned accuracy, it was required to calculate the power series up to $n=255$ in (4.15) and (4.16) for $Fr=7$ and $k=10$, which was the greatest n and the number of the iterations is about 20~40.

In principle, it is possible to locate a zero point of f to any accuracy by repeating the procedure (c) without using (d). There is another way to evaluate directly the value of C by an integral

$$C=\frac{1}{2\pi i}\oint_L \frac{C'}{f(C')}\frac{df}{dC'}dC'\,, \tag{4.21}$$

which can be applied to any (not necessarily small) closed contour L encircling the zero point. However, it turned out that both of the methods are less convenient compared with the simplest trial and error method described in (d). Efficiencies of the methods may depend on types of problems and also on details of numerical calculations.

Results of the eigenvalue calculations are presented in Figs. 3 and 4. Figs. 3(a) and 3(b) show the phase speeds C_r and growth rates kC_i for $Fr=5$, respectively. The meanings of the indices (1,1), (1,2), etc. are explained later. Figs. 4(a) and 4(b) are the same as Figs. 3(a) and 3(b) respectively, except for $Fr=7$. Both Figs. 3(a) and 4(a) are symmetric about the line $C_r=0.5$, as expected from the symmetry of the model.

Inspecting Figs. 3(a) and 4(a), we notice that the k-C_r relation (dispersion relation) has particular features. They might be interpreted as follows. If we assume that the basic flow is constant, equation (4.9) has solutions of simple gravity waves and their dispersion relation is given as

$$C=u_0\pm\frac{1}{Fr}\sqrt{1+\frac{(n\pi)^2}{k^2}}\,, \tag{4.22}$$

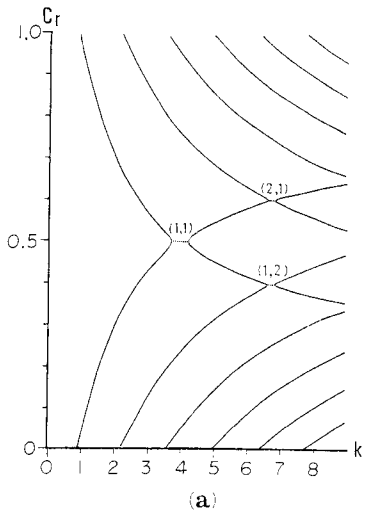

Fig. 3(a) Curves of non-dimensional phase velocity for $Fr=5$ and case I. Solid lines are neutral modes and dotted lines are growth modes.

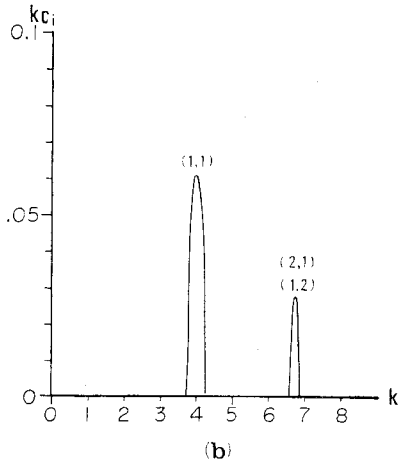

Fig. 3(b) Curves of non-dimensional growth rate for $Fr=5$.

where u_0 is the velocity of the constant basic flow and the factor $n\pi$ comes from the boundary conditions at two rigid walls. We may assume, to a first approximation, that the waves are advected by the mean speed of the basic flow. Thus, we take $u_0=1/2$ in this case and have approximate dispersion relations for the two families as

$$C_+^{(n)}=\frac{1}{2}+\frac{1}{Fr}\sqrt{1+\frac{(n\pi)^2}{k^2}}, \qquad (4.23a)$$

$$C_-^{(n)}=\frac{1}{2}-\frac{1}{Fr}\sqrt{1+\frac{(n\pi)^2}{k^2}}. \qquad (4.23b)$$

These relations are shown schematically in Fig. 5(a).

At the next step, we consider distortion of the phase speeds by the basic flow which varies with y. For the sake of simplicity U is assumed to change slowly. Then (4.9) is approximated as

$$\frac{d^2\hat{h}}{dy^2}=-k^2\{Fr^2(y-C)^2-1\}\hat{h}. \qquad (4.24)$$

Now, for the family of the faster phase speeds $C_-^{(n)}$ $(>1/2)$, the value in the bracket of (4.24) has greater positive values near the wall at $y=0$ than near the wall at $y=1$: and a region of negative value of the bracket, where the solutions cannot be sinusoidal but becomes exponential, appears (for $Fr\geq 2$) near the wall at $y=1$. Thus, the solutions are more wavy near $y=0$ than $y=1$ and the area where the solutions are sinusoidal

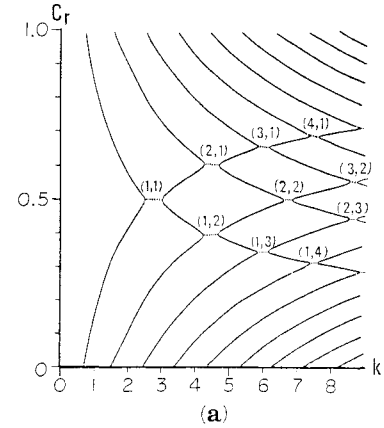

Fig. 4(a) Same as Fig. 3(a), except for $Fr=7$.

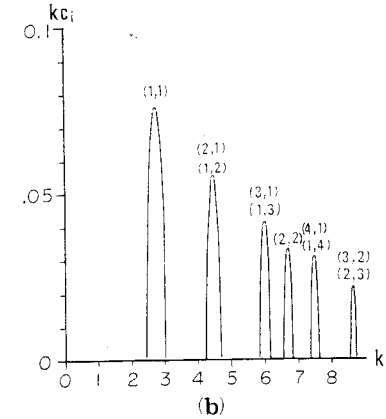

Fig. 4(b) Same as Fig. 3(b), except for $Fr=7$.

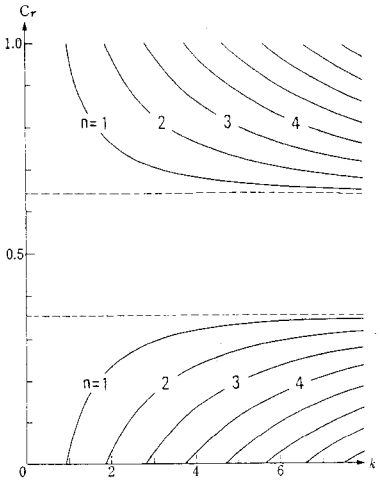

(a)

Fig. 5(a) Dispersion relations for $C_+^{(n)}$ and $C_-^{(n)}$. Upper dashed line is $C_r=0.5+Fr^{-1}$ and lower one is $C_r=0.5-Fr^{-1}$.

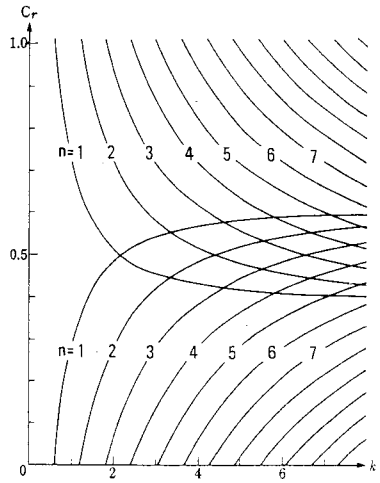

(b)

Fig. 5(b) Dispersion relations for modified $C_+^{(n)}$ and $C_-^{(n)}$.

is larger near $y=0$ than $y=1$*. Then we may consider that the family of $C_+^{(n)}$ has more energy near $y=0$ than $y=1$ and that they are advected not by the mean speed $u_0=1/2$ but by the basic flow at a point closer to $y=0$, *i.e.*, by a speed $u_-^{(n)}<1/2$. For the family of the slower phase speeds $C_-^{(n)}$, the effect of the basic shear is reversed and they may be advected by a speed $u_+^{(n)}>1/2$. Then, (4.23) may be rewritten as

$$C_+^{(n)}\sim u_-^{(n)}+\frac{1}{F_r}\sqrt{1+\frac{(n\pi)^2}{k^2}}, \qquad (4.25a)$$

$$C_-^{(n)}\sim u_+^{(n)}-\frac{1}{F_r}\sqrt{1+\frac{(n\pi)^2}{k^2}}. \qquad (4.25b)$$

Above relations are shown schematically in Fig. 5(b). Fig. 5(b) is very similar to Figs. 3(a) or 4(a). In general, if two neutral modes cross in the k-C_r plane, *i.e.*, if a degeneracy occurs, it is expected that phase speed C becomes complex-valued near the crossing point (see, *e.g.*, Gustavsson *et al.* 1980), and it really occurs as shown in Figs. 3(a) and 4(a).

From the above discussion we interpret that eigen-solutions shown in Figs. 3 and 4 are essentially gravity waves modified and destabilized by the basic shear flow.

Now, the meanings of the indices (1,1), (1,3), etc. in Figs. 3 and 4 are clear. The first index in brackets indicates the number, n, of the faster phase speed mode expressed by (4.25a) and the second index indicates that of (4.25b). The two modes are mixed to produce this unstable mode. Thus, for example, (1,2) means the unstable mode whose parents are the $C_+^{(1)}$ mode and the $C_-^{(2)}$ mode.

Next, we shall look into the structure of unstable waves. Figs. 6(a), 6(b), 6(c) and 6(d) show amplitude of h for the (1,1), (2,2), (2,1) and (3,2) modes for $Fr=7$, respectively. As understood from the previous discussion, a mode (n_1, n_2) has n_1 maxima near $y=0$ and n_2 maxima near $y=1$.

Fig. 7 shows the amplitudes of the divergence and the vorticity for (1,1) mode of $Fr=7$. We

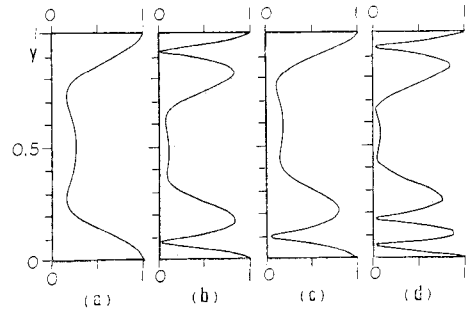

Fig. 6 Amplitude of non-dimensional surface displacement h for $Fr=7$ and case I. (a) $k=2.75$, $Cr=0.5$ and $kCi=0.076$ (mode (1,1)). (b) $k=6.7$, $Cr=0.5$ and $kCi=0.033$ (mode (2,2)). (c) $k=4.45$, $Cr=0.6$ and $kCi=0.054$ (mode (2,1)). (d) $k=8.65$, $Cr=0.55$ and $kCi=0.021$ (mode (3,2)).

* This supposition will be verified by the structures of the eigensolutions as shown in Fig. 6.

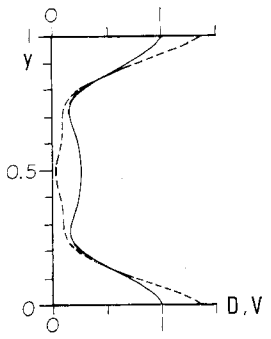

Fig. 7 Amplitude of divergence (D) and Vorticity (V) for $Fr=7$, $k=2.75$, $Cr=0.7$ and $kCi=0.076$ (mode (1,1) in case I). Solid line is the vorticity and dashed line is the divergence.

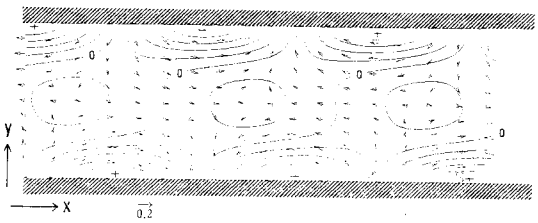

Fig. 8 Structure of the unstable wave for the same parameters as Fig. 7. Solid lines are contours of h and arrows denote velocity (u, v). Contour interval is 0.2.

see that the divergence is greater than the vorticity near the boundary, where both of them attain maxima. This fact can be an evidence that these unstable waves are of gravity wave origin.

Fig. 8 illustrates the structure of the unstable wave. This structure is very similar to that of gravity wave in a channel, especially near the boundaries (structure of a gravity wave is shown in Appendix). As shown in Fig. 8, the wave crest has a tilt; the phase at a larger y point leads that at a small y, possibly owing to differential advection by the basic shear flow. Examining the relationship between h and u we notice that the wave tends to move toward the left side ($x<0$) near the $y=1$ boundary while near the $y=0$ boundary the wave has a structure to move to the right, if there is no basic flow. Since the basic flow has a shear which just opposes the above mentioned motions arising from the wave structure, this structure can be maintained. Inspecting the velocity field closely, we notice that u and v are negatively correlated in the middle part of the channel. Thus there is a down-gradient transport of the zonal momentum and hence the disturbance gains energy from the mean field as seen from (3.19). It is interesting that this negative uv correlation is a result of the tilt of the wave as mentioned before, because the velocity vector tends to be perpendicular to an equal phase line (or it is parallel with the wave number vector), which is a property of gravity waves. If the disturbances were of rotation type, the same tilt of equal phase line would be accompanied by a positive $\overline{uv}$ and hence the wave would decay. Thus we know that this unstable wave owes its existence to the gravity wave mechanisms.

We will call these unstable waves as SG-waves.

4.3 *Case II: Plane Couette flow bounded in one side*

Next we consider a fluid which is bounded by a rigid wall at $y=1$ but extends to $y\to-\infty$. The basic flow is

$$U(y)=\begin{cases} y & 0\leq y\leq 1 \quad \text{(region I)}, \\ 0 & y\leq 0 \quad \text{(region II)}, \end{cases} \tag{4.26}$$

and boundary conditions are

$$v=h'=0 \quad \text{at} \quad y=1, \tag{4.27}$$

and the perturbation quantities remain finite as $y\to-\infty$ or radiate to $y\to-\infty$.

The interfacial boundary condition is that the velocity component normal to the internal boundary and the surface displacement h should be continuous at $y=0$,

$$v_{\mathrm{I}}=v_{\mathrm{II}}, \quad h_{\mathrm{I}}=h_{\mathrm{II}} \quad \text{at } y=0, \tag{4.28}$$

where suffices I and II denote those quantities belonging to the regions I and II, respectively. This situation is schematically shown in Fig. 9.

In region I (shear zone), the posed problem is the same as case I except for the boundary condition at $y=0$; the governing equation in region I is the same as (4.9) and its solution is expressed as

$$\hat{h}=A_{\mathrm{I}}\sum_{n=3(\mathrm{odd})}^{\infty}a_n z^n+B_{\mathrm{I}}\sum_{n=2(\mathrm{even})}^{\infty}a_n z_n\,. \tag{4.29}$$

Above equation is the same form as (4.12) but constants A_I and B_I are determined from the boundary conditions (4.27) and (4.28).

In region II (rest fluid), equation (2.6) is written as

$$\frac{d^2\hat{h}}{dy^2}+k^2(Fr^2C^2-1)\hat{h}=0\,, \tag{4.30}$$

and its solution is

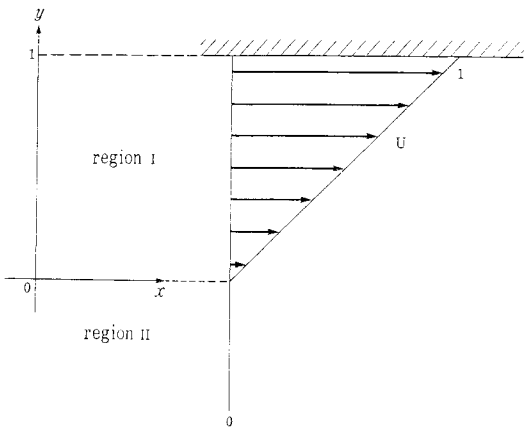

Fig. 9 The model in case II. Fluid extends to $y\to-\infty$. Shear zone (region I) is $0\leq y\leq 1$ and rest fluid (region II) is $y\leq 0$.

$$\hat{h}_{\mathrm{II}}=A_{\mathrm{II}}\exp(k\sqrt{1-F_r^2C^2}\,y)+B_{\mathrm{II}}\exp(-k\sqrt{1-F_r^2C^2}\,y)\,, \tag{4.31}$$

where A_{II} and B_{II} are constants. From the boundary condition at $y\to-\infty$, $\hat{h}_{II}$ should have a form as

$$\hat{h}_{\mathrm{II}}=A_\beta e^{\beta y} \tag{4.32}$$

where A_β is a constant and

$$\beta=\begin{cases}-ik\sqrt{F_r^2C^2-1} & \text{for } F_r^2C^2\geq 1\,, \quad (4.33a)\\ k\sqrt{1-F_r^2C^2} & \text{for } F_r^2C^2\leq 1\,, \quad (4.33b)\end{cases}$$

Of course, the right-hand side of (4.33a) gives the same value as what (4.33b) gives in the case where C has an imaginary part.

The interfacial boundary condition for v is equivalent to the continuity of h'. Thus, using (4.29) and (4.32), boundary conditions (4.28) are rewritten as

$$\beta A_\beta=A_{\mathrm{I}}\sum_{n=3(\mathrm{odd})}^{\infty}na_n(-C)^{n-1}+B_{\mathrm{I}}\sum_{n=0(\mathrm{even})}na_n(-C)^{n-1}\,, \tag{4.34}$$

and

$$A_\beta=A_{\mathrm{I}}\sum_{n=3(\mathrm{odd})}^{\infty}a_n(-C)^n+B_{\mathrm{I}}\sum_{n=2(\mathrm{even})}^{\infty}a_n(-C)^n. \tag{4.35}$$

From (4.34) and (4.35), we eliminate A_β to obtain

$$A_{\mathrm{I}}\sum_{n=3(\mathrm{odd})}^{\infty}(n+\beta C)a_n(-C)^{n-1}+B_{\mathrm{I}}\{\beta+\sum_{n=3(\mathrm{odd})}^{\infty}(n+\beta C)a_n(-C)^{n-1}\}=0\,. \tag{4.36}$$

Substituting (4.29) into (4.27), we obtain another relation between A_I and B_I as

$$A_{\mathrm{I}}\sum_{n=3(\mathrm{odd})}^{\infty}na_n(1-C)^{n-1}B_{\mathrm{I}}\sum_{n=2\ (\mathrm{even})}^{\infty}na_n(1-C)^{n-1}=0\,. \tag{4.37}$$

Requiring that A_I and B_I do not vanish, we have a characteristic equation for C as

$$F(k,F_r;C)=\begin{vmatrix}F_1 & F_2\\ F_3 & F_4\end{vmatrix}=0\,, \tag{4.38}$$

where

$$F_1=\sum_{n=3(\mathrm{odd})}^{\infty}(n+\beta C)a_n(-C)^{n-1}\,,$$

$$F_2=\sum_{n=2(\mathrm{even})}^{\infty}na_n(1-C)^{n-1}\,,$$

$$F_3=\beta+\sum_{n=3(\mathrm{odd})}^{\infty}(n+\beta C)a_n(-C)^{n-1}$$

$$F_4=\sum_{n=3(\mathrm{odd})}^{\infty}na_n(1-C)^{n-1}\,.$$

Equation (4.38) is solved by the same method that as used in case I to the same accuracy.

Results of the eigenvalue calculations are presented in Figs. 10, 11 and 12. Figs. 10(a) and 10(b) show the phase speeds C_r and the growth rates kC_i for $Fr=3.5$, respectively. Figs. 11(a) and 11(b) are the same as Figs. 10(a) and 10(b) respectively, except for $Fr=5$. Figs. 12(a) and 12(b) are the same as Figs. 10(a) and 10(b) respectively, except for $Fr=7$. From these figures, it is easily found that there are two different types of unstable waves: one is fast to move and slow to grow, and the other is slow to move and fast to grow. We will call the latter unstable waves as SG_1-waves and former ones as SG_2-waves.

Comparing Figs. 10, 11, and 12 with Figs. 3 and 4, we also notice that these k-C_r relations have similar characteristics with each other. They may be interpreted as follows. When the wall at $y=0$ is removed, almost all members of the family of the faster phase speed $C_+^{(n)}$ may disappear, because they have more energy near that wall and they may be greatly affected by the wall. On the other hand the family of $C_-^{(n)}$ may not be modified remarkably because they have more energy near the wall at $y=1$ which exists in this case, too. But some parts of them whose phase speeds exceed the value $C_r=1/Fr$ can not remain to be neutral, because they radiate to $y\to-\infty$ as the boundary condition (4.33a) shows, that is momentum is lost to infinity and thus energy conversion may occur. Thus the phase

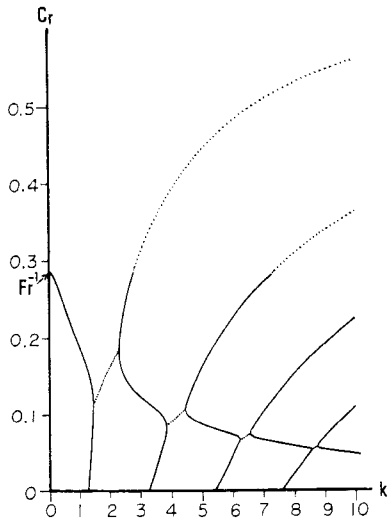

(a)

Fig. 10(a) Curves of non-dimensional phase velocity for $Fr=3.5$ in case II. Solid lines are neutral modes and dashed lines are growth modes.

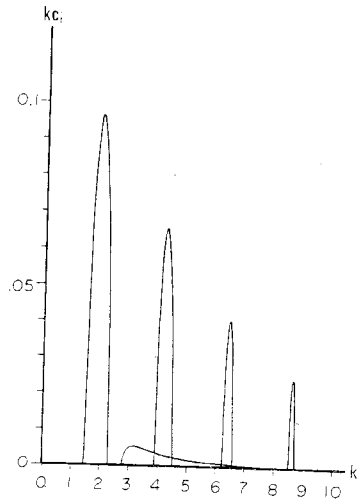

(b)

Fig. 10(b) Curves of non-dimensional growth rate for $Fr=3.5$. Rather discrete curves and continuously extended curves correspond SG_1-waves and SG_2-waves, respectively.

speeds must have complex values in that upper region of the k-C_r plane. On these grounds, SG_2-waves may be interpreted as the destabilized part of the wave family $C_-^{(n)}$ while SG_1 may correspond to $(1, n)$ modes, where $n=1, 2, 3, \ldots$, in the last subsection, though the reason why only the $(1, n)$ could survive is not clear. Indeed, SG_1-waves have a second maximum of the surface displacement h as a trace of the energy concentration near $y=0$ as shown in Fig. 15, which is a characteristic of the family of $C_+^{(n)}$.

There exist the most unstable wave near $Fr=3.5$. When Fr becomes greater or smaller (not shown) than 3.5, the growth rate is reduced.

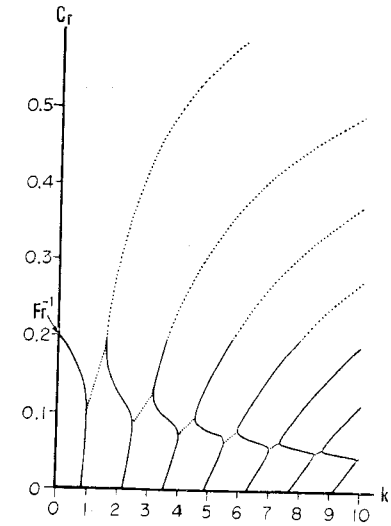

(a)

Fig. 11(a) Same as Fig. 10(a), except for $Fr=5$.

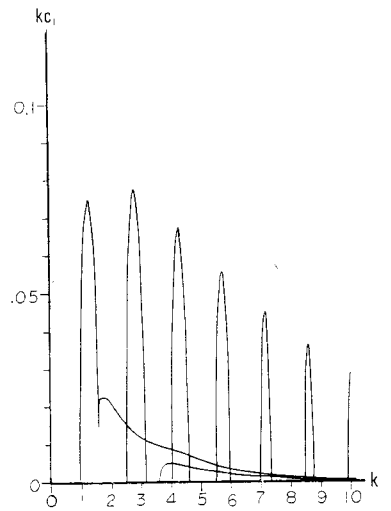

(b)

Fig. 11(b) Same as Fig. 10(b), except for $Fr=5$.

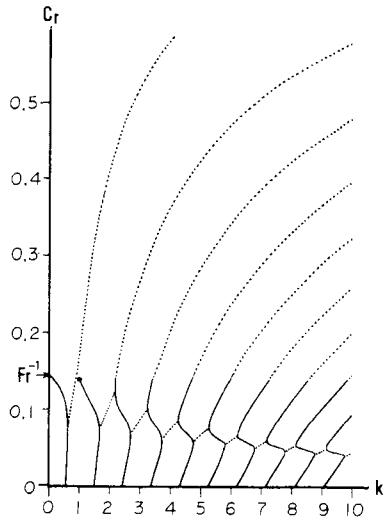

(a)

Fig. 12(a) Same as Fig. 10(a), except for $Fr=7$.

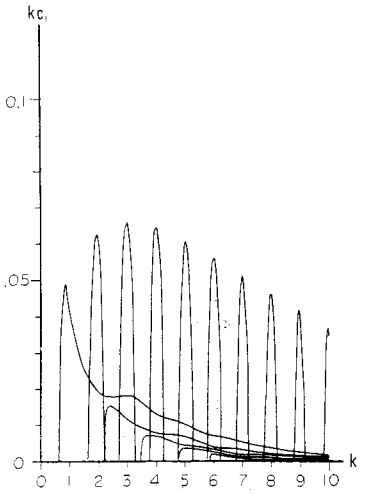

(b)

Fig. 12(b) Same as Fig. 10(b), except for $Fr=7$.

When Fr increases, all unstable waves shift to the longer wavelength side and the phase speeds of SG_1-waves and SG_2-waves become closer as shown in Fig. 11. Finally ($Fr=7$), these two unstable regions of the ground modes are joined together completely as shown in Fig. 12. Simultaneously, the neutral solution vanishes at the branch point of the solution, $FrC=1$. This vanishing point is denoted by a small circle in Fig. 12(a).

Fig. 13 shows the divergence and the vorticity

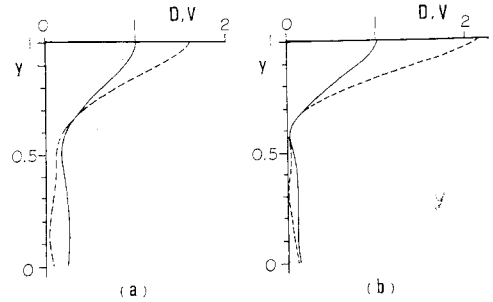

Fig. 13 Amplitude of non-dimensional divergence and vorticity for $Fr=3.5$ in Case II. Solid lines are the vorticity and dashed lines are the divergence. (a) $k=1.9$, $Cr=0.155$ and $kCi=0.096$ (SG_1-waves). (b) $k=3.1$, $Cr=0.319$ and $kCi=0.005$ (SG_2-wave).

of the perturbation velocity at $Fr=3.5$. The modes which are shown in Fig. 13(a) and 13(b) correspond to the ground mode of the SG_1-waves and SG_2-waves, respectively. It is evident that divergence is dominant near the boundary for both two waves.

To verify that these unstable waves are destabilized gravity waves, the vorticity equation and the divergence equation are derived from (2.2)~(2.4). Then we estimate the amplitudes of the terms in these equations. The vorticity equation is written as

$$\frac{\partial \zeta}{\partial t}+U\frac{\partial \zeta}{\partial x}+\bar{\zeta}D=0\,, \tag{4.39}$$

and the divergence equation is written as

$$\frac{\partial D}{\partial t}+U\frac{\partial D}{\partial x}+2\frac{\partial v}{\partial x}\frac{dU}{dy}+\frac{1}{Fr^2}\nabla^2 h=0\,, \tag{4.40}$$

where ζ is the perturbation vorticity $\partial v/\partial x-\partial u/\partial y$, $\bar{\zeta}$ is the basic vorticity $-dU/dy$, D is the perturbation divergence and

$$\nabla^2=\frac{\partial^2}{\partial x^2}+\frac{\partial^2}{\partial y^2}\,.$$

The results of the calculation are shown in Fig. 14. From this figure, following points are observed:

(a) Near the boundary, the second term and the last term of (4.39) almost cancel each other. It means that vorticity variation due to stretching of vortex tube by the divergence maintains the wave structure against the advection by the fast basic flow.

(b) Near the boundary, the sum of the first and the second terms of (4.40) balances the last term. This is a characteristics of gravity waves,

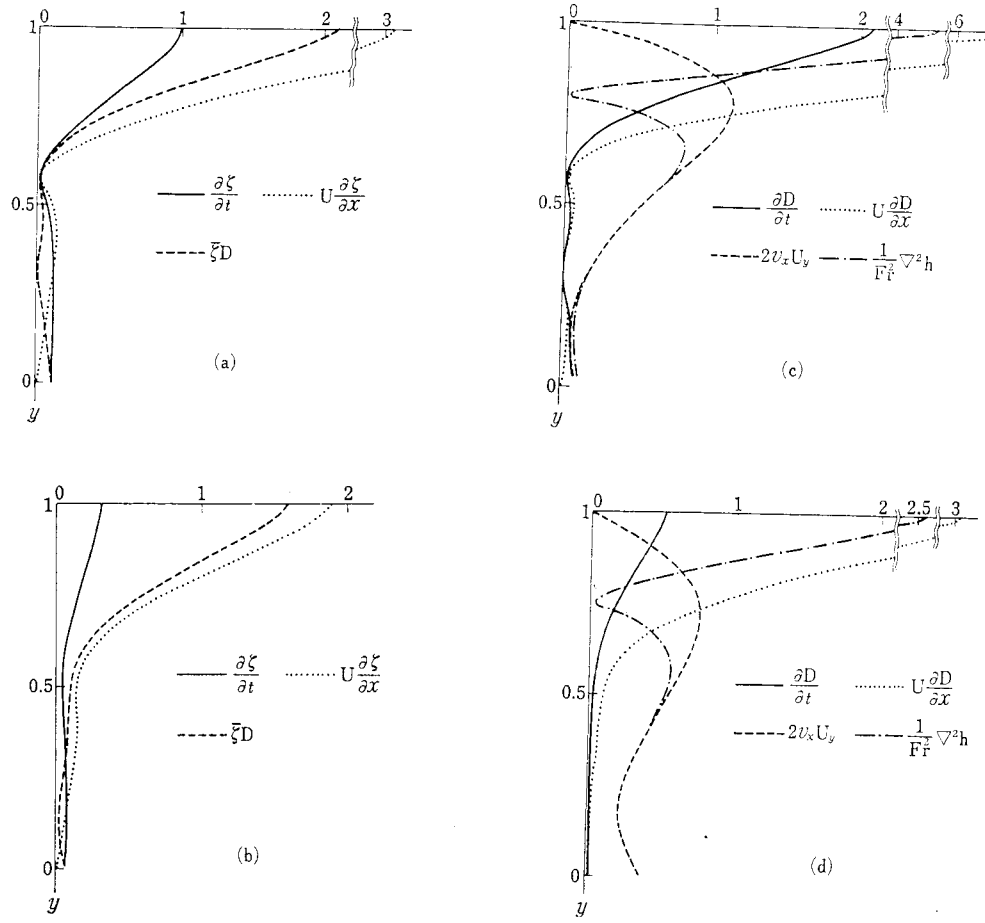

Fig. 14 Absolute values of each term of the vorticity equation and the divergence equation. (a) Absolute values of terms of the vorticity equation for SG_1-wave. Parameters are same as Fig. 13(a). (b) Same as (a) except for SG_2-waves and parameters which are same as Fig. 13(b). (c) Same as (a) except for the terms of the divergence equation. (d) Same as (b) except for the terms of the divergence equation.

Fig. 15(a) and 15(b) depict the structures of the ground modes of the SG_1-waves and the SG_2-waves for $Fr=3.5$, respectively. As already mentioned, these figures clearly show that the SG_2-wave radiates to $y\rightarrow-\infty$ as gravity wave, while the SG_1-wave quickly damps away from the interface. Near the boundary at $y=1$, the structure of either wave is similar to that of a gravity wave in a channel. The waves also have desired forms appropriate to match the requirement of maintaining themselves against the basic shear flow as explained in the case I.

5. Potential vorticity budget, change of zonal mean flow, and energetics

In this section, we will show an interesting aspect of the disturbance in linear shear flows.

From (3.20) and (3.21), it is obvious that disturbances extract their energy from the zonal mean kinetic energy through the conversion term due to the Reynolds stress. In the case of the linear shear, however, this conversion term is expressed as (4.5). From a comparison between (4.5), (3.21), and (3.22) we see that the 'ordinary' zonal mean kinetic energy E_B must not change, and that the perturbation quantities can grow at the expense of the additional energy term E_{BP}, and thus reduce the 'depth weighted' zonal mean kinetic energy E_S. This is a difference from usual barotropically unstable waves. In order to make this difference clearer, the tendency of U with time is calculated from that of the basic potential

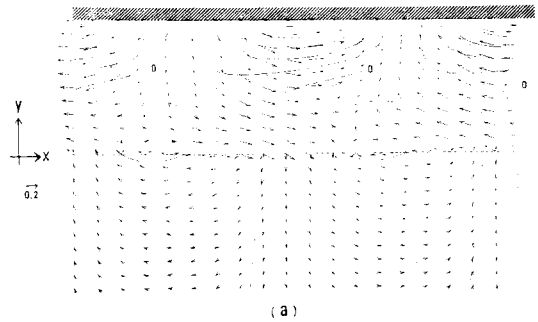

Fig. 15(a) Structure of the perturbation quantities in case II. Parameters are the same as Fig. 13(a) and $\beta=1.65-0.21i$. Solid lines are contour of h and arrows are velocity (u, v). Contour interval is 0.2.

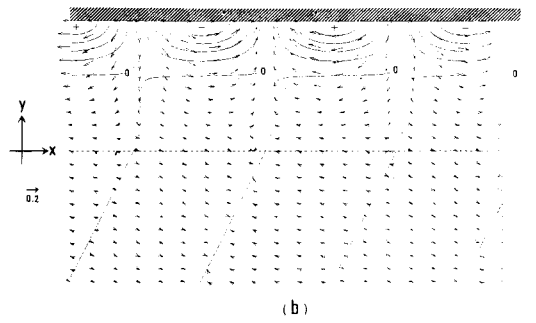

Fig. 15(b) Same as Fig. 15(a), except for $\beta=0.04-1.55i$ and the parameters which are the same as Figs. 13(b).

vorticity and of the depth H. To do this, we use the expansion (3.11) again and also assume that the second order variables $U^{(2)}$, $V^{(2)}$, and $H^{(2)}$ are independent on x.

Then, potential vorticity Q may be expanded as

$$\begin{aligned} Q&=\frac{\dfrac{\partial v^{\dagger}}{\partial x}-\dfrac{\partial u^{\dagger}}{\partial y}}{h^{\dagger}} \\ &=\frac{\varepsilon\dfrac{\partial v}{\partial x}-\left(\dfrac{dU}{dy}+\varepsilon\dfrac{\partial u}{\partial y}+\varepsilon^2\dfrac{\partial U^{(2)}}{\partial y}\right)}{H+\varepsilon h+\varepsilon^2 H^{(2)}} \\ &=-\frac{1}{H}\frac{dU}{dy}+\frac{\varepsilon}{H}\left(\frac{\partial v}{\partial x}-\frac{\partial u}{\partial y}+\frac{h}{H}\frac{dU}{dy}\right) \\ &\quad+\frac{\varepsilon^2}{H^2}\left[-h\left(\frac{\partial v}{\partial x}-\frac{\partial u}{\partial y}+\frac{h}{H}\frac{dU}{dy}\right)\right. \\ &\quad\left.+H^{(2)}\frac{dU}{dy}-H\frac{\partial U^{(2)}}{\partial y}\right]+0(\varepsilon^3)\,. \end{aligned} \tag{5.1}$$

On the other hand, the equation of the conservation of the potential vorticity,

$$\frac{\partial Q}{\partial t}+u^{\dagger}\frac{\partial Q}{\partial x}+v^{\dagger}\frac{\partial Q}{\partial y}=0 \tag{5.2}$$

is derived from the original equations for $u^{\dagger}$, $v^{\dagger}$,

Substituting (3.11) and (5.1) into (5.2), arranging each power of ε and note that first order quantities to have the form as (2.5), then we obtain (in the linear shear zone),

$$Q^{(1)}=0\,, \tag{5.3}$$

$$\frac{\partial Q^{(2)}}{\partial t}=\frac{\partial\overline{Q^{(2)}}}{\partial t}=0\,, \tag{5.4}$$

where

$$\left.\begin{aligned} Q&=Q^{(0)}+\varepsilon Q^{(1)}+\varepsilon^2\left(\overline{Q^{(2)}}-\frac{h}{H}Q^{(1)}\right) \\ Q^{(0)}&=-\frac{1}{H}\frac{dU}{dy} \\ Q^{(1)}&=\frac{1}{H}\left(\frac{\partial v}{\partial x}-\frac{\partial u}{\partial y}+\frac{h}{H}\frac{dU}{dy}\right) \\ Q^{(2)}&=\frac{1}{H^2}\left(H^{(2)}\frac{dU}{dy}-H\frac{\partial U^{(2)}}{\partial y}\right) \end{aligned}\right\} \tag{5.5}$$

Physically the above results are rather obvious. Since the basic potential vorticity is uniform, no potential vorticity can accompany the disturbance as seen from (5.3). Then the disturbance cannot cause any change of the zonal mean vorticity field through the non-linear effect as shown in (5.4). In the case of a non-divergent flow (*e.g.* barotropic instability problem), it means that the zonal mean flow and the kinetic energy associated with it do not change at all; hence disturbances do not grow. In the present problem, we have a somewhat strange situation as explained below. For convenience, we rewrite (5.4) as

$$\frac{\partial}{\partial t}\frac{\partial U^{(2)}}{\partial y}=\frac{1}{H}\frac{dU}{dy}\frac{\partial H^{(2)}}{\partial t}\,. \tag{5.6}$$

Now, upon using (2.5) and the condition that $V^{(2)}$ should be zero at the walls or $y\to-\infty$ for unstable waves, (3.19) is rewritten as

$$\frac{\partial H^{(2)}}{\partial t}=-\frac{\partial\overline{hv}}{\partial y}\,. \tag{5.7}$$

Substitute (5.7) into (5.6) and integrate with respect y to obtain

$$\frac{\partial U^{(2)}}{\partial t}=-\frac{1}{H}\frac{dU}{dy}\overline{hv}+G(t)\,, \tag{5.8}$$

where $G(t)$ is a function of time only, and we used the fact that dU/dy is a constant in the

shear zone. For convenience, we consider the situation in case I, then, from the symmetry of the model, $G(t)$ should be zero. Then from (5.7) and (5.8) we have

$$\frac{\partial}{\partial t}(HU^{(2)}+H^{(2)}U)=-\frac{\partial}{\partial y}(U\overline{hv}). \qquad (5.9)$$

This implies that the zonal mean momentum may change, despite the fact that $Q^{(2)}$ does not change. However, if the perturbation disappears at the final stage, U should return to the initial distribution, because $Q=$const. Then 'zonal mean acceleration by waves' does not take place in the present problem. However if we consider $\overline{hu}$ as a part of the zonal mean momentum, it can change as mentioned previously (cf. 3.21 and 3.22). Redistribution of physical quantities such as momentum or mass by the waves may be one of the interests of instability problems. Although the unstable waves found in this paper have strange characteristics in their energetics, they have a possibility to redistribute the momentum of the basic flow. To show this, assume the situation that the energy conversion from the basic flow to the perturbation is compensated by the energy loss due to viscosity which is considered to act only on the perturbation vorticity, but not to affect the surface displacement h. (So far we consider an initial tendency of the effect of the viscosity, these assumptions may have no great difficulty, because the viscosity affect the surface displacement h not directly but through the change of velocity field.) From these assumptions and (5.1), the tendency of the second order potential vorticity may be written as

$$\begin{aligned}\frac{\partial Q^{(2)}}{\partial t}&=\frac{1}{H}\frac{\partial}{\partial t}h\overline{Q^{(1)}}\\&=\frac{1}{H^2}\overline{\zeta h}+\frac{1}{H^3}\frac{dU}{dy}\frac{\partial\overline{h^2}}{\partial t}\\&=\frac{1}{H^2}\frac{\partial}{\partial t}\overline{\zeta h}, \qquad (5.10)\end{aligned}$$

where the constancy of h with time is used. Since the basic vorticity $-dU/dy$ is negative, the stretching of the vortex tube by the h creates negative vorticity. Thus a correlation between h and ζ may be negative, and

$$\frac{\partial}{\partial t}\overline{\zeta h}>0, \qquad (5.11)$$

because dissipation reduces the absolute value of the perturbation vorticity. Substituting (5.11) into (5.10), we obtain an inequality

$$\frac{\partial}{\partial t}\overline{Q^{(2)}}>0. \qquad (5.12)$$

With the fact that $Q^{(0)}=-(1/H)(dU/dy)<0$, above inequality implies that the absolute value of the basic potential vorticity will be reduced. It means that the basic shear will be weakened and the redistribution of the momentum can occur.

From another point of view, this redistribution is also suggested. The perturbation momentum $\overline{hu}$ is calculated from the eigenfunction and is found to be negative near $y=1$ ($U=U_{\max}$) and is positive near $y=0$ ($U=U_{\min}$). Then, the basic shear will decrease, if we assume that the waves will be dissipated by viscosity but the perturbation momentum will remain where it is.

Of course, to prove strictly what are discussed above, a finite amplitude theory with the effect of the viscosity should be required. We do not extend our discussion to the finite amplitude theory.

The right-hand side of (5.8) is calculated explicitly and it is shown schematically in Fig. 16. From Fig. 16 only, it seems as if the 'ordinary' mean kinetic energy E_B will decrease. The energetics shows, however, E_B must be constant with time. This apparent contradiction may be avoided by considering the variation of the mean surface, $H^{(2)}$, because definition of E_B includes that effect. This is also shown as follows: The explicit form of the left-hand side of (3.23a) is

$$\frac{\partial}{\partial t}\int\frac{1}{2}(H^{(2)}U^2+2HUU^{(2)})dy. \qquad (5.13)$$

Substituting (4.8a) and (5.7) into (5.13), and integrating by parts to rewrite the left-hand side

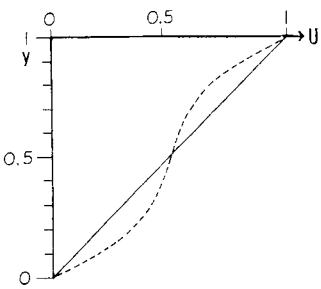

Fig. 16 The tendency of the variation of the basic flow. Solid line is the basic flow, U, and dashed line is the modified basic flow $U+\varepsilon^2U^{(2)}$. But the value of ε is set to be arbitrary large for convenience to show the effect of $U^{(2)}$.

of (3.23a) as

$$\frac{\partial}{\partial t}\int E_B dy = \int y\left(\overline{hv}+H\frac{\partial U^{(2)}}{\partial t}\right)dy\,. \qquad (5.14)$$

Equation (5.8) implies that the right-hand side (5.14) should be zero. Thus, even if the zonal mean shear changes as in the case of barotropic instability, the compensating effect by the elevation of the mean surface will make the 'ordinary' mean kinetic energy E_B unchange.

6. Summary and discussions

Using an analytical solution of the linearized forms of the shallow water equations, we have studied the stability of plane Couette flows.

The characteristics of unstable waves are summarized:

(a) In the case I, there are unstable gravity waves (SG-waves). The instability occurs in discrete intervals of the zonal wave number, and they are interpreted to be produced as a result of the mixing of two gravity wave modes which would propagate opposite directions if the basic flow did not exist. A strong shear ($Fr\geq 2$) can cause the mode mixing.

(b) In the case II, there exist two different types of unstable waves. One is the almost trapped but radiating waves; part of their energy radiates to $y\rightarrow -\infty$ (SG_2-waves). The other is the trapped waves (SG_1-waves). The SG_2-waves are interpreted as destabilized parts of a family of waves which are neutral in the case I. The SG_1-waves are interpreted as one of the unstable wave series in the case I modified by the unbounded fluid.

(c) Near the boundaries, the vorticity pattern of the SG, SG_1 and SG_2-waves are maintained by stretching and shrinking of the vortex tube due to the divergence. In the divergence equation, these waves show the characteristics of gravity waves near the boundaries.

(d) These SG, SG_1 and SG_2-waves obtain their energy from the 'additional" mean energy $\overline{hu}U$ and not from the 'ordinary' mean energy $1/2\,H^{(2)}U^2+HUU^{(2)}$.

(e) Perturbation potential vorticity equals zero, and the mean potential vorticity does not change with time.

These instabilities does not change the 'ordinary' mean kinetic energy ~~or momentum~~.

The SG_2-waves might be the same, in essence, as the unstable waves which are found by Broadbent and Moore (1979) and the second mode of Blumen *et al.* (1975). But, since Broadbent *et al.* (1979) discussed neither structures nor energetics sufficiently, similarity between the two waves is not so obvious. In addition to this vagueness of the similarity, they found unstable waves even in the case where Mach number $M<1$. The reason why subsonic flow is unstable is not so clear. Their model is compressible homoentropic fluid, and they used the cylindrical coordinates and assumed that the basic vortex has uniform vorticity in the core and zero outside the core. This means that a pressure gradient along the radial direction exists and it corresponds to an inclination of the undisturbed surface in our shallow water model. We only suppose that these differences might break our necessary condition (4.7).

In view of our results which show that gravity waves are unstable for $Fr>1$ even without a point of inflection, the second mode of Blumen *et al.* (1975) may be interpreted as unstable accoustic waves which are similar to ours and have little connection with the point of inflection essentially. In order to connect our results with theirs straightforwardly, we examined the stability of the basic flow which has a profile as

$$U(y)=\begin{cases} 1 & 1\leq y \\ y & 0\leq y\leq 1 \\ 0 & y\leq 1 \end{cases}. \qquad (6.1)$$

The results of the calculations of the eigenvalues verify the above interpretation. But, in contrast with the results of Blumen *et al.*, the high wave number cut off of the second unstable mode in k-Fr plane is not found in this model. Further results of this model will be presented elsewhere.

Our instabilities are found only for $Fr>1$. It should be noted that possibility of meeting this condition in actual geophysical fluids is expected rather large, because, in a stably stratified fluid, the mean depth of the shallow water, H, may be replaced by the vertical scale of the waves, H_s, and thus $Fr=U_0/NH_s$, where N is the Brunt-Välsälä frequency. Thus defined Fr may be able to exceed 1. In concluding the paper, the author wishes to mention one interesting application. In the upper atmosphere of Venus where the 4-day circulation is dominant, a shear in the angular velocity is expected to exist (cf. Matsuda, 1980), and those unstable waves may exist. Indeed, if we use a model as

$$U(y)=\begin{cases} y & 0\leq y\leq 1 \\ -y & -1\leq y\leq 0 \end{cases}, \qquad (6.2)$$

with boundary conditions

$$v=0 \quad \text{at} \quad y=1 \quad \text{and} \quad y=-1\,, \qquad (6.3)$$

eigenfunctions will be symmetric about the line $y=0$. Thus the pattern in the domain $0\leq y\leq 1$ is the same as Fig. 8 and the other half is a mirror image of it with respect the line $y=0$. This looks like the Y shape disturbance in the Venus atmosphere (see, for example, Belton *et al.* 1976). Further, the tilting of the equal brightness contour of this disturbance is the same direction of the shear of the angular velocity. Thus this disturbance may not be of a rotational motion type but a gravity wave type, as pointed in the last part of the subsection 4–2. Here we only point out the similarity between their shapes. Further comparison is left for a study using a more realistic spherical model. If the unstable waves found in this paper exist, they may be a mechanism of large horizontal eddy viscosity which is assumed in some models of the 4-day circulation (*e.g.* Gierasch, 1975; Matsuda, 1980).

Acknowledgements

The author is greatly indebted to Dr. T. Matsuno for leading the author into this problem, useful discussions, encouragements, and careful readings of the manuscript. He wishes to thank other staffs in Meteorological Laboratory of Tokyo University and Dr. M. Miyata in Laboratory of Physical Oceanography for useful discussions. He is also grateful to Mrs. K. Kudo who typed the manuscript.

The computations were performed with the use of a HITAC 8700/8800 computer at the Computer Center of Tokyo University and a FACOM M-190 computer at the LICEPP which belongs to Tokyo University.

Appendix: Gravity waves in a channel

Here we derive structures of neutral gravity waves in a channel for reader's convenience for comparing with the structures of the unstable waves which is found in this paper.

Shallow water equations for gravity waves in a rest fluid are written as

$$\frac{\partial u}{\partial t}+g\frac{\partial h}{\partial x}=0\,,$$
$$\frac{\partial v}{\partial t}+g\frac{\partial h}{\partial y}=0\,, \qquad (A.1)$$
$$\frac{\partial h}{\partial t}+H\left(\frac{\partial u}{\partial x}+\frac{\partial v}{\partial y}\right)=0\,.$$

Eliminating u and h from (A.1), we obtain single equation for v as

$$\frac{d^2\hat{v}}{dy^2}=-k^2(c^2-gH)\,\hat{v}, \qquad (A.2)$$

where all perturbation quantities are assumed to have a form as (2.5). Boundary conditions are

$$v=0 \quad \text{at} \quad y=0 \quad \text{and} \quad y=L\,, \qquad (A.3)$$

where L is a channel width.

Then dispersion relation is obtained as

$$c=\pm\sqrt{gH}\sqrt{1+\frac{(n\pi)^2}{L^2k^2}}\,. \qquad (A.4)$$

and u, v, and h are obtained as

$$u=A\frac{in\pi\cos(n\pi y/L)}{Lk\{1-(c^2/gH)\}}e^{ik(x-ct)}\,,$$
$$v=A\sin\frac{n\pi}{L}y\,e^{ik(x-ct)}\,, \qquad (A.5)$$
$$h=A\frac{icn\pi\cos(n\pi y/L)}{Lk\{1-(c^2/gH)\}}e^{ik(x-ct)}\,,$$

where A is a constant.

Results of the calculation of the structure by (A.5) are shown in Fig. A1.

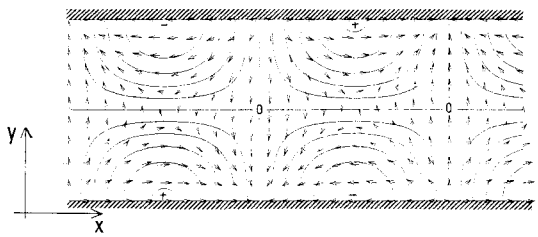

Fig. A1 Structure of neutral gravity wave. Solid lines are contours of h and arrows are velocity (u, v). Contour interval is 0.2.

References

Belton, M. J. S. and G. R. Smith, 1976: Cloud patterns, waves and convection in the Venus atmosphere. *J. Atmos. Sci.*, **33**, 1394–1417.

Blumen, W., 1970: Shear layer instability of an inviscid compressible fluid. *J. Fluid Mech.*, **40**, 769–781.

————, 1971: Hydrostatic neutral waves in a parallel shear flow of a stratified fluid. *J. Atmos. Sci.*, **28**, 340–344.

Blumen, W., P. G. Drazin and D. F. Billings, 1975: Shear layer instability for an inviscid compressible fluid. Part 2. *J. Fluid Mech.*, **71**, 305–316.

Broadbent, E. G., and D. W. Moore, 1979: Acoustic destabilization of vortices. *Proc. Roy. Soc. London*, **A290**, 353–371.

Case, K. M., 1960: Stability of inviscid plane Couette flow. *Phys. Fluid.*, **3**, 143–148.

Fjørtoft, R., 1950: Application of integral theorems in deriving criteria of stability for laminar flows and for the baroclinic circular vortex. *Geofys. publ.*, **17**, 1–52.

Gierasch, P., 1975: Meridional circulation and the maintenance of Venus atmospheric rotation. *J. Atmos. Sci.*, **32**, 1038–1044.
Gustavsson, L. H. and L. S. Hultgren, 1980: A resonance mechanism in plane Couette flow. *J. Fluid Mech.*, **98**, 149–159.
Howard, L. N., 1961: Note on a paper of John W. Miles. *J. Fluid Mech.*, **10**, 509–512.
Kurihara, Y., 1976: On the development of spiral band in a tropical cyclone. *J. Atmos. Sci.*, **33**, 940–958.
Lipps, F. B., 1963: Stability of jets in a divergent barotropic fluid. *J. Atmos. Sci.*, **20**, 120–129.
Matsuda, Y., 1980: Dynamics of the four-day circulation in the Venus atmosphere. *J. Meteor. Soc. Japan*, **58**, 443–470.
Philander, S. G. H., 1976: Instabilities of zonal equatorial current. *J. Geophys. Res.*, **81**, 3725–3735.
Willoughby, H. E., 1977: Inertia-buoyancy waves in hurricanes. *J. Atmos. Sci.*, **34**, 1028–1039.
————, 1978: A possible mechanism for the formation of hurricane band. *J. Atmos. Sci.*, **35**, 838–848.

浅水のシヤー不安定に関する研究

里　村　雄　彦
東京大学理学部地球物理学教室

シヤーのある平行流の線型安定性を浅水方程式を用いて調べた。この方程式系における不安定の必要条件とHoward の半円定理を導き，エネルギー交換について論じたのち，次の2種の平行流の安定性を吟味した。即ち，両側に壁がある平行 Coutte 流と片側に無限大まで続く静止流体が接続している Coutte 流である。方程式の確定特異点付近の冪級数の形に解を表現することによって，固有関数と固有値を精度良く求めた。

両側に壁がある場合，フルード数が2以上で重力波が不安定になった。フルード数を固定したとき，波数に関して離散的に不安定となる。片側に静止流体が続く場合にはフルード数が1以上で2種の不安定重力波があった。ひとつは壁付近に束縛された波で前の場合の不安定波の変形と解釈される。もうひとつはエネルギーを無限遠へ放射する波で，前の場合には中立波であったモードである。

これらの不安定波は深さを重みとして平均した運動エネルギーからエネルギーを引き出すことを示した。不安定波による運動量再配分の可能性についても議論した。